



## Adsorbent material from pomegranate (*Punica granatum*) leaves: Optimization on removal of methylene blue using response surface methodology

Malak EDDEBBAGH<sup>1\*</sup>, Abdelmjid ABOURRICHE<sup>1</sup>, Mohamed BERRADA<sup>1</sup>,  
Mourad BEN ZINA<sup>2</sup> and Ahmed BENNAMARA<sup>1</sup>

<sup>1</sup> Laboratory ' Biomolecules and Synthesis Organique ', Faculty of Sciences Ben M'Sick, University Hassan II Casablanca, B.P 7955, Casablanca, Morocco.

<sup>2</sup> Laboratory of Water, Energy and Environment (LR3E), National School of Engineers of Sfax, University of Sfax, 6 B.P1173.W.3038 Sfax, Tunis

Received 02 Dec 2015, Revised 11 Apr 2016, Accepted 19 Apr 2016

\*Corresponding author. E-mail: [malak.eddebbagh@yahoo.fr](mailto:malak.eddebbagh@yahoo.fr) (M.Eddebbagh); Phone:+212 666352889

### Abstract

Pomegranate (*Punica granatum*) leaves are an important source of potentially healthy bioactive compounds and according to our study, activated carbon prepared from leaves of pomegranate has become an excellent organic pollutant and heavy metals adsorbent. An experimental setup based on the Central Composite Design (CCD) with three factor interaction was implemented in order to optimizing the conditions for the preparation of this adsorbent material. The effects of the activation temperature, activation time, and chemical impregnation ratios on the carbon yield and Methylene Blue (MB) removal were investigated. The optimum conditions for preparing activated carbon from leaves of pomegranate were found to be activation temperature of 723°K, activation time of 2h 24min, and chemical impregnation ratio of 1.45. The carbon yield was found to be 60.6% while the removal of MB was found to be 90.5%.

**Keywords:** Pomegranate leaves, Activated carbon, Methylene Blue, Central composite design, Optimization.

### 1. Introduction

The twentieth century was characterized by considerable technical progress, accompanied by an unprecedented population boom, these two factors that the global water consumption increased from 400 to 7000 billion, 32% are the requirements to Industry [1]. Hazardous and toxic noxious waste, such as dyes and/or phenolics, are chemically stable against natural degradation and mostly found in industrial effluents. Dyes are a large group of organic compounds that are used in various fields, such as food, textiles, cosmetics, and chemical processes [2]. The failure to provide safe drinking water and adequate sanitation services to all people is perhaps the greatest development failure of this century. If no action is taken to address unmet basic human needs for water, as many as 135 million people will die from water-related diseases by 2020 [3].

MB has wider applications, which include coloring paper, temporary hair colorant, dyeing cottons, wools and coating for paper stock [4]. The harmful effects of MB include: breathing difficulties, nausea, vomiting, tissue necrosis, profuse sweating, mental confusion, cyanosis and methemoglobinemia. MB has been widely employed as a model cationic dye in adsorption studies, using low-cost adsorbents such as natural minerals (clays, zeolites and perlite), activated carbon, agricultural and industrial wastes [5].

Activated carbons are famous because they possess outstanding adsorption characteristics due to their improved pore structures. Therefore, activated carbon is the most widely used adsorbent material for the treatment of industrial wastewaters due to its efficiency and economic feasibility. The ability of activated carbons to adsorb

pollutants from aqueous solutions depends on two major factors: experimental conditions of the activation processes and the nature of organic material utilized for the preparation of activated carbon [6, 7].

Several studies investigate the optimal conditions for preparation of activated carbons, for removal of dyes like from mangosteen peel for removal of Remazol Brilliant Blue R (RBBR) [8], rubber seed coat for removal of Malachite Green (MG) [9], waste tea for adsorption of MB and Acid Blue29 (AB29) [10], periwinkle shell for removal of RBBR [11], residues of marine sponges for removal of MB [12], and for adsorption of heavy metals like from pomegranate wood for adsorption of copper (II) [13], from sugarcane bagasse for chromium (VI) sorption [14], and for removal of pesticides from palm oil fronds [15], also Optimizing the production of microporous activated carbon from waste palm shell was done for flue gas desulphurization [16].

The focus of this research is to evaluate the adsorption potential of pomegranate leaves based activated carbon for Methylene Blue. MB was chosen in this study because of its known strong adsorption onto solids and it often serves as a model compound for removing organic contaminants. Thus, an experimental design methodology with three factor interaction was implemented in order to optimizing the conditions for the preparation of this new adsorbent material.

## 2. Materials and Methods

### 2.1. Preparation of dye solution

Methylene Blue (fig. 1) is a cationic dye with molecular formula  $C_{16}H_{18}N_3S^+Cl^-$ , molar weight of 319.85 g/mol and wave length of  $\lambda_{max} = 664$  nm. This cationic dye presents high water solubility at 293 °K and is positively charged on S atom [17 and 18]. The stock solutions of MB were prepared in distilled water. All working solutions were prepared by diluting the stock solution with distilled water to the needed concentration. Fresh dilutions were used for each adsorption study.

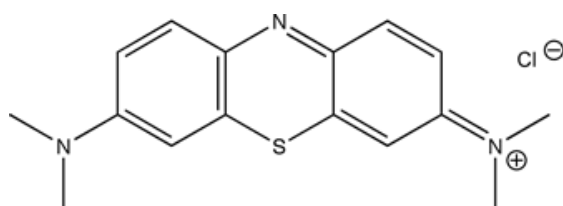


Figure 1. Chemical structure of methylene blue

### 2.2. Preparation of Activated Carbon

*Punica granatum* leaves were collected in January 2014 from Berrechid (Municipality of Chaouia-Ouardigha) region (33 ° 16'12 "North, 7 ° 34'59 " West). The precursor was first washed to remove dirt from its surface and was then dried in an oven at 383 K for 2h and pulverised in a domestic blender. The dried precursor was mixed with activating agent with different impregnation ratio (x), as calculated using:

$$x = W_{\text{agent}} / W_{\text{precursor}} \quad (1)$$

The obtained pastas mixture was then dehydrated in an oven overnight at 393 K to remove moisture and was then activated under the same condition as carbonization. The activated product was then cooled to room temperature and then washed with hot distilled water until all acid was eliminated, dried, ground and sifted to obtain a powder with a particle size capable of passing through a 100 $\mu$ m sieve. The domains of variation of activation temperature, activation time and percentage of chemical activated agent were defined on the univariate analysis.

### 2.3. Univariate analysis

Univariate analysis is the first step of analysis of process variables because she explores each variable in a data set, separately. Temperature (T) (523 – 873 K), time (t) (30min - 5h) and impregnation ratio (x) (0.5 - 3). The analysis is carried out with the description of a single variable and its attributes of the applicable unit of analysis. This step was used in the first stages of research, in analyzing the data at hand, before being supplemented by multivariate analysis using experimental design.

#### 2.4. Experimental design

A central composite design (CCD) is the most commonly used response surface methodology (RSM) and is effective for minimizing the number of runs required to develop the model, evaluating the effects of several variables, and searching for the optimized response [19]. JMP statistical software was utilized to identify the most influential factor on each experimental design response. The activated carbons were prepared using the chemical activation method by varying the preparation variables using the CCD. The three independent variables or factors studied were T [ $x_1$ , varying between 723 and 823 K], t ( $x_2$ , varying between 2 and 4h) and x ( $x_3$ , varying between 1.25 and 1.75). Each variable to be optimised was coded at three levels, -1, 0 and 1 (Table 1). The three independent variables were coded according to the following equation:

$$x_i = \frac{X_i - X_0}{\Delta X_i}, \quad x_i = 1, 2, 3 \quad (2)$$

Where  $x_i$  and  $X_i$  are the dimensionless and the actual value of the independent variable  $i$ ,  $X_0$  the actual value of the independent variable  $i$  at the central point and  $\Delta X_i$  the step change of  $X_i$  corresponding to a unit variation of the dimensionless value. These three variables together with their respective ranges were chosen based on the literature and preliminary studies. Activation temperature, activation time and chemical impregnation ratio are the important parameters affecting the characteristics of the activated carbons produced [15 and 20]. The total number of experimental trials ( $n_e$ ) depends on the number of factors and the number of center points ( $n_c$ ). The total number of experimental trials is expressed in following equation [21 and 22]:

$$n_e = 2^k + 2k + n_c \quad (3)$$

The number of experimental runs from the central composite design (CCD) for the three variables consists of eight factorial points, six axial points and two replications the center points indicating that altogether 16 experiments were required, as calculated from Eq. (3):  $n_e = 2^3 + 2 \times 3 + 2 = 16$ .

The experimental sequence was randomized in order to minimize the effects of the uncontrolled factors. The two responses ( $Y_1$ ) were activated carbon yield and dye removal ( $Y_2$ ). Each response was used to develop an empirical model which correlated the response to the three preparation process variables using a second degree polynomial equation as given by Eq. (4):

$$Y = a_0 + \sum_{i=1}^n a_i x_i + \sum_{i=1}^n a_{ii} x_i^2 + \sum_{i=1}^{n-1} \sum_{j=i+1}^n a_{ij} x_i x_j \quad (4)$$

Where  $Y$  is the predicted activated carbon yield or the removal response,  $a_0$  the constant coefficient,  $a_i$  the linear coefficient,  $a_{ij}$  the interactions coefficients,  $a_{ii}$  the quadratic coefficient and  $x_i$  and  $x_j$  are the coded values of the activated carbon preparation or MB removal variables [6, 15 and 23].

#### 2.5. Determination of responses

##### 2.5.1. Adsorbent material yield

The experimental activated carbon yield was calculated based on the following equation (4), where  $w_c$  and  $w_0$  are the dry weight of final activated carbon (g) and dry weight of precursor (g), respectively:

$$Y_1 = \text{AC Y \%} = \frac{w_c}{w_0} \times 100 \quad (5)$$

##### 2.5.2. Capacity of adsorption

The biosorption experiments of MB on pomegranate leaf carbon adsorbent were carried out in batch method. For each experimental run, 100 mL of dye solution of known concentration and a known amount of the adsorbent were taken in a 200 mL stoppered conical flask. This mixture was agitated at laboratory temperature at a constant speed of 120 rpm. Samples were withdrawn at different time intervals (0–240 min), filtrated and analyzed for remaining dye concentration. The concentration of MB in solution was analyzed using UV spectrophotometer by monitoring the absorbance at a wavelength 664 nm. The percentage removal of dye at equilibrium was calculated by the following equation (6):

$$Y_2 = \text{MB R \%} = \frac{C_0 - C_t}{C_0} \times 100 \quad (6)$$

Where  $C_0$  and  $C_t$  (mg/L) are dye initial concentration and dye concentration at time  $t$  respectively [24].

#### 2.6. Characterization of raw material and Activated Carbon

X-ray powder diffraction analysis of the adsorbent was carried out using a Philips® PW 1710 diffractometer (Cu  $K\alpha$ , 40 kV/40 mA, scanning rate of  $2\theta$  per min).

The functional groups on the surface of the precursor and activated carbon were determined by FTIR spectroscopy. The spectra were recorded using a NICOET spectrophotometer. The spectrum was obtained over the range of 400-4000  $\text{cm}^{-1}$ .

Thermogravimetric analysis of the raw material and activated carbon was performed in a Perkin-Elmer TG/DTA apparatus at a nitrogen flow rate of 100 ml/min and a heating rate of 283 K/min up to 873 K.

$S_{\text{BET}}$  surface areas of the solids were measured by nitrogen adsorption at 77 K using a Micrometitics ASAP 2010 analyzer.

The morphology of the samples was studied using scanning electronic microscopy (SEM, Hitachi SU-70).

### 3. Results and discussion

#### 3.1. Univariate analysis

After determining the preliminary range of extraction variables through single-factor test, a three-level-three-factor, central composite design (CCD) was employed in this optimization study. Extraction temperature ( $x_1$ ), extraction time ( $x_2$ ) and impregnation ratio ( $x_3$ ) were the independent variables selected to be optimized for the preparation of activated carbon. The range of independent variables and their levels were presented in Table 1.

**Table 1.** Independent variables and their coded levels for the central composite design.

Variables (factors)	Code	Units	Levels		
			-1	0	+1
Activation temperature T	$x_1$	K	723	773	823
Activation time t	$x_2$	min	120	180	240
Impregnation ratio x	$x_3$	-	1.25	1.5	1.75

#### 3.2. Development of regression model equation

A central composite design (CCD) was used to develop a polynomial regression equation in order to identify the relationship existing between the response functions and process variables as well as to determine those conditions that optimised the extraction process. Table 2 shows the complete design matrixes together with both the response values obtained from the experimental work. Run 15 and 16 at the center point were conducted to determine the experimental error and the reproducibility of the data. According to the sequential model sum of squares, the models were selected based on the highest order polynomials where the additional terms were significant and the models were not aliased. For both responses of MB removal and AC yield, the quadratic models were selected as suggested by the software. The final empirical models in terms of coded factors (parameters) for the activated carbon yield (Y) and MB removal (R) are represented by Eq. (7) and (8), respectively:

$$Y = 58.043017 - 5.705x_1 - 1.269x_2 - 11.393x_3 - 11.86078x_1^2 + 7.1092241x_2^2 + 2.3592241x_3^2 + 4.355x_1x_2 + 2.185x_1x_3 + 5.2375x_2x_3 \quad (7)$$

$$R = 85.127586 - 8.034x_1 - 5.524x_2 + 4.316x_3 + 7.9286207x_1^2 - 2.966379x_2^2 - 55.341379x_3^2 - 8.37625x_1x_2 - 0.40125x_1x_3 - 3.24875x_2x_3 \quad (8)$$

The coefficient with one factor represent the effect of the particular factor, while the coefficients with two factors and those with second-order terms represent the interaction between two factors and quadratic effect, respectively. The positive sign in front of the terms indicates synergistic effect, whereas negative sign indicates antagonistic effect [8]. The accuracy of the model developed can be understood by the value of  $R^2$  and standard deviation.  $R^2$  indicates the ratio between sum of the squares (SSR) with total sum of the square (SST) and it describes up to what extent perfectly the model estimated experimental data points. The standard deviation is defined as the square root of the variance. In fact, the models developed seems to be the best at low standard deviation and high  $R^2$  statistics which is closer to unity as it will give predicted value closer to the actual value for the responses [25]. In this experiment, the  $R^2$  values for Eq. (7) and (8) were 0.903 (Fig. 2) and 0.956 (Fig. 3), respectively. The standard deviations for the two models were 12.829 and 11.765 for Eq. (7) and (8), respectively. The  $R^2$  of 0.903 for Eq. (7) was considered relatively high, indicating that the predicted values for activated carbon yield would be more accurate and closer to its actual value. The  $R^2$  of 0.956 for Eq. (8) was

considered high, indicating that there was an agreement between the experimental and the predicted in the MB removal of the activated carbon. The relatively low value of standard deviation for MB removal and AC yield also indicates that the predicted values for both models were considered as suitable to correlate the experimental data. The adequacy of the models was further justified through analysis of variance (ANOVA). The performance of the model can be observed by the plots of predicted versus experimental percentage by Fig. 2 and 3.

**Table 2.** Experimental design matrix for preparation of activated carbon from pomegranate leaves

Run	Levels			Activated Carbon preparation variables			Activated Carbon Yield Y%	MB Removal R%
	x <sub>1</sub>	x <sub>2</sub>	x <sub>3</sub>	Activation temperature (K)	Activation time (min)	Impregnation ratio		
1	0	+α	0	773	240	1.5	58.33	74.13
2	0	0	0	773	180	1.5	54.89	90.15
3	-α	0	0	723	180	1.5	51.06	98.41
4	+1	+1	+1	823	240	1.75	52.86	64.25
5	+1	+1	-1	823	240	1.25	55.00	62.50
6	-1	+1	+1	723	240	1.75	44.30	98.41
7	0	0	0	773	180	1.5	56.67	89.75
8	-1	+1	-1	723	240	1.25	70.92	94.25
9	0	0	+α	773	180	1.75	54.28	80.05
10	+1	-1	-1	823	120	1.25	63.83	83.35
11	-1	-1	+1	723	120	1.75	49.60	98.75
12	-1	-1	-1	723	120	1.25	81.43	82.40
13	+α	0	0	823	180	1.5	43.57	82.88
14	+1	-1	+1	823	120	1.75	30.00	98.90
15	0	-α	0	773	120	1.5	74.24	85.38
16	0	0	-α	773	180	1.25	68.79	74.70

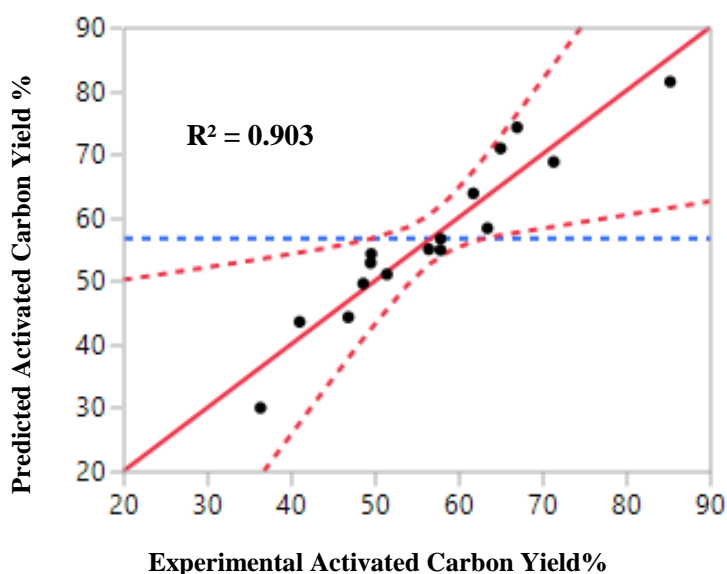


**Figure 2.** Predicted versus experimental Activated Carbon Yield %.

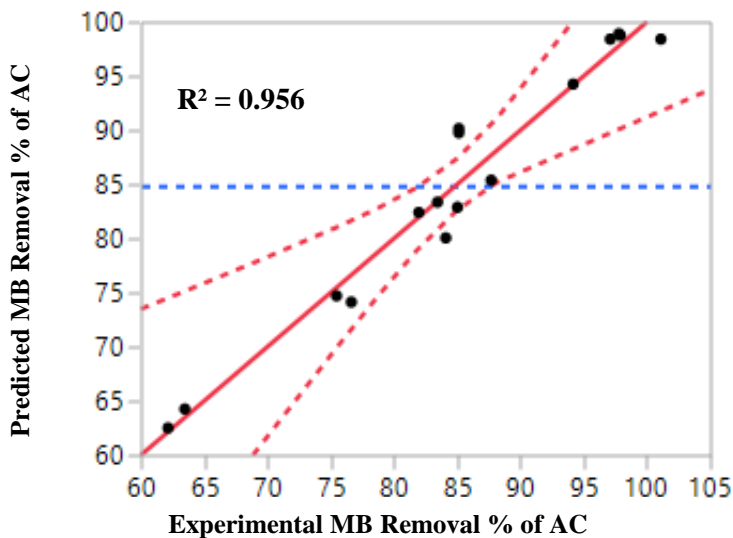


Figure 3. Predicted versus experimental MB Removal % of AC.

### 3.3. Analysis of variance

The analysis of variance (ANOVA) is a general statistical technique for partitioning and analyzing the variation in a continuous response variable [26]. In fact, the ANOVA is a sign whether the regression equation adequately represents the relationship between the response and significant variables. The ANOVA was further studied to justify the adequacy of model [27]. The ANOVA for the quadratic polynomial model of activated carbon Yield and MB Removal are listed in table 3 and 4, respectively.

Table 3. Analysis of variance for response surface quadratic polynomial model of activated carbon Yield

Source	Sum of Square	DF	Mean Square	Fvalue	Pvalue
Model	2229.53	9	247.50	6.211	0.019
x <sub>1</sub>	270.92	1	270.92	6.796	0.0403
x <sub>2</sub>	31.294	1	31.294	0.785	0.409
x <sub>3</sub>	1186.57	1	1186.6	29.765	0.0016
x <sub>1</sub> x <sub>2</sub>	111.303	1	111.30	2.792	0.146
x <sub>1</sub> x <sub>3</sub>	63.169	1	63.169	1.585	0.255
x <sub>2</sub> x <sub>3</sub>	170.20	1	170.20	4.269	0.084
x <sub>1</sub> <sup>2</sup>	354.88	1	354.88	8.902	0.0245
x <sub>2</sub> <sup>2</sup>	143.115	1	143.11	3.59	0.107
x <sub>3</sub> <sup>2</sup>	18.067	1	18.067	0.453	0.526
Residual	239.189	6	39.865	-	-
Lack of fit	237.613	5	47.523	30.167	0.137
Pure error	1.575	1	1.575	-	-

From the ANOVA from table 3 and 4, for response surface quadratic model for activated carbon Yield and MB Removal, respectively the model *F*-value of 6.21 and 14.44 implied that the model was significant. *F*-values of *P*-values less than 0.05 indicated that the model terms were significant [27 and 29]. A test for lack-of-fit indicating the significance of the replicate error in comparison to the model dependent error can be performed. The test statistic for lack-of-fit is the ratio between the lack-of-fit mean square and the pure error mean square. Insignificant lack-of-fit is desired as significant lack-of-fit indicates that there might be contributions in the regressor-response relationship that are not accounted for by the model [28 and 29]. In this experiment, *F*-value for the lack of fit for the quadratic polynomial model of AC Yield and MB Removal was insignificant (*P* > 0.05) thereby confirming the validity of the model [30].

**Table 4.** Analysis of variance for response surface quadratic polynomial model of Methylene Blue Removal

Source	Sum of Square	DF	Mean Square	Fvalue	Pvalue
Model	1984.53	9	220.5	14.436	0.002
$x_1$	645.451	1	645.451	42.258	0.0006
$x_2$	305.146	1	305.146	19.978	0.0042
$x_3$	186.278	1	186.278	12.196	0.013
$x_1 x_2$	561.292	1	561.292	36.748	0.0009
$x_1 x_3$	1.288	1	1.288	0.0843	0.781
$x_2 x_3$	84.435	1	84.435	5.528	0.0570
$x_1^2$	165.73	1	165.73	10.85	0.0165
$x_2^2$	23.198	1	23.198	1.519	0.264
$x_3^2$	75.216	1	75.216	4.924	0.068
Residual	91.64	6	15.274	-	-
Lack of fit	91.654	5	18.313	228.91	0.0501
Pure error	0.080	1	0.080	-	-

The regression coefficient values of Eq. (7) and Eq. (8) were listed in Table 3 and 4 for response surface quadratic model for activated carbon Yield and MB Removal, respectively. The P-values were used as a tool to check the significance of each coefficient, which in turn might indicate the pattern of the interaction between the variables. The smaller the value of P was, the more significant the corresponding coefficient was [30]. It can be seen from table 3 of activated carbon yield, that just the linear coefficients ( $x_1$  and  $x_3$ ) and a quadratic term coefficient  $x_1^2$  were significant, with small P-values ( $P < 0.05$ ). The other term coefficients were not significant ( $P > 0.05$ ). And from table 4 of MB Removal, that the linear coefficients ( $x_1$ ,  $x_2$  and  $x_3$ ), a quadratic term coefficient  $x_1^2$  and the interaction term  $x_1x_2$  were significant, with very small P-values ( $P < 0.05$ ) whereas  $x_2^2$ ,  $x_3^2$ ,  $x_1x_3$  and  $x_2x_3$  were insignificant to the response. The full model fitted Eq. (7) and Eq. (8) were made three-dimensional and contour plots to predict the relationships between the independent variables and the dependent variable.

### 3.4. Process Optimization

One of the main aims of this study was to find the optimum process parameters which AC prepared should have a high carbon yield and a high MB removal. However, it is difficult to optimize both these responses under the same condition because the interest region of factors is different. When adsorption performance increases, carbon yield will decrease and vice versa. Therefore, the function of desirability was applied using Design-Expert software in order to compromise between these two responses. Shown in figure 4, in the optimization analysis, the target criteria was set as maximum values for the two responses of AC yield (Y) and MB removal (R) while the values of the three variables were set in the ranges being studied.

According to Fig. 2 and above single parameter study, it can be concluded that optimal preparation conditions of activated carbon were extraction temperature 723 K, extraction time 144 min and impregnation ratio of phosphoric acid to raw material 1.45. At those recommended settings it was predicted with 95% confidence that the average Y% and R% would be  $60.82 \pm 10.96\%$  and  $96.76 \pm 6.79\%$  respectively. For activated carbon yield, among the three parameters studied, the ratio of phosphoric acid to raw material was the most significant factor to affect this response of pomegranate leaves activated carbon, followed by extraction temperature and extraction time was insignificant according to the regression coefficients significance of the quadratic polynomial model (Table 3) and gradient of slope in the 3-D response surface plot in Figure 5.

For methylene blue removal, the temperature was the most significant factor to affect this response of pomegranate leaves activated carbon, followed by extraction time and ratio of phosphoric acid to raw material according to the regression coefficients significance of the quadratic polynomial model (Table 4) and gradient of slope in the 3-D response surface plot in Figure 6.

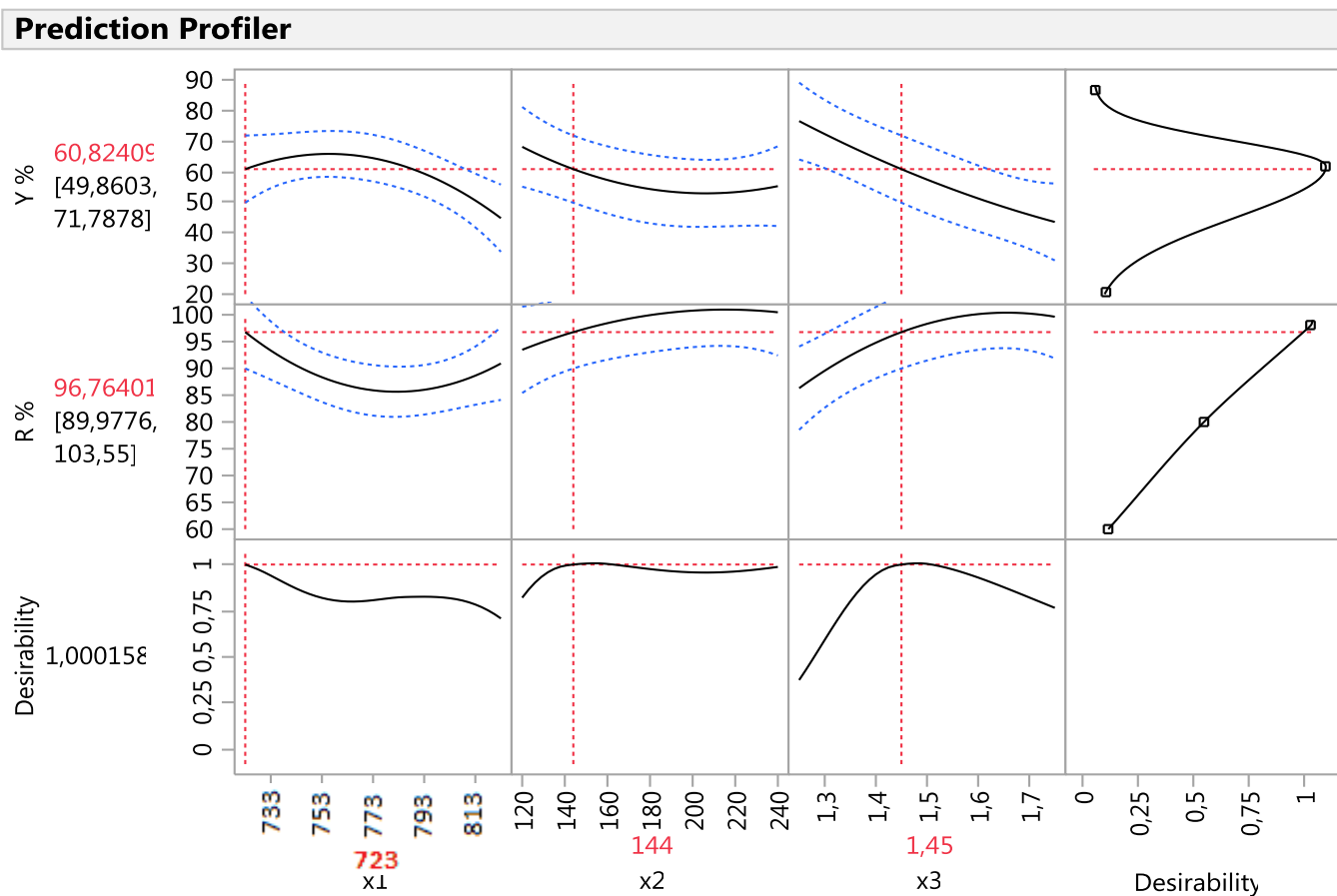


Figure 4. Prediction profiler that displays the models and settings contributing in achieving the overall maximum desirability

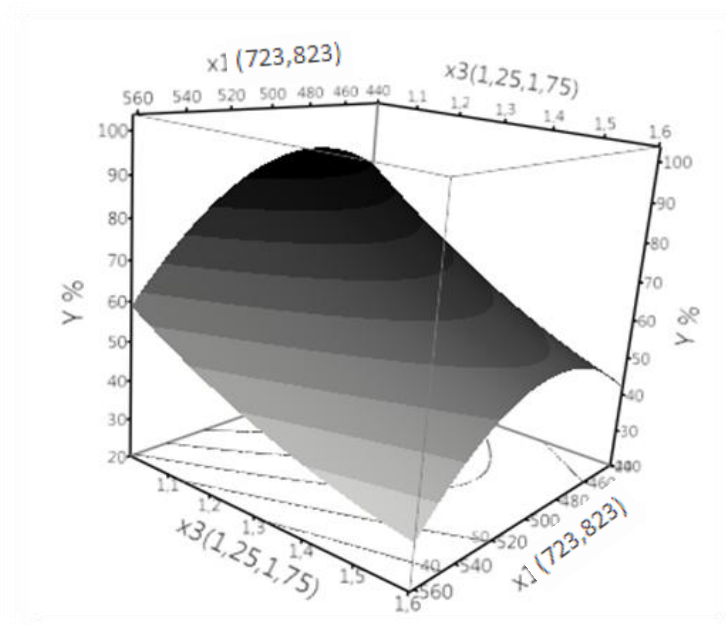
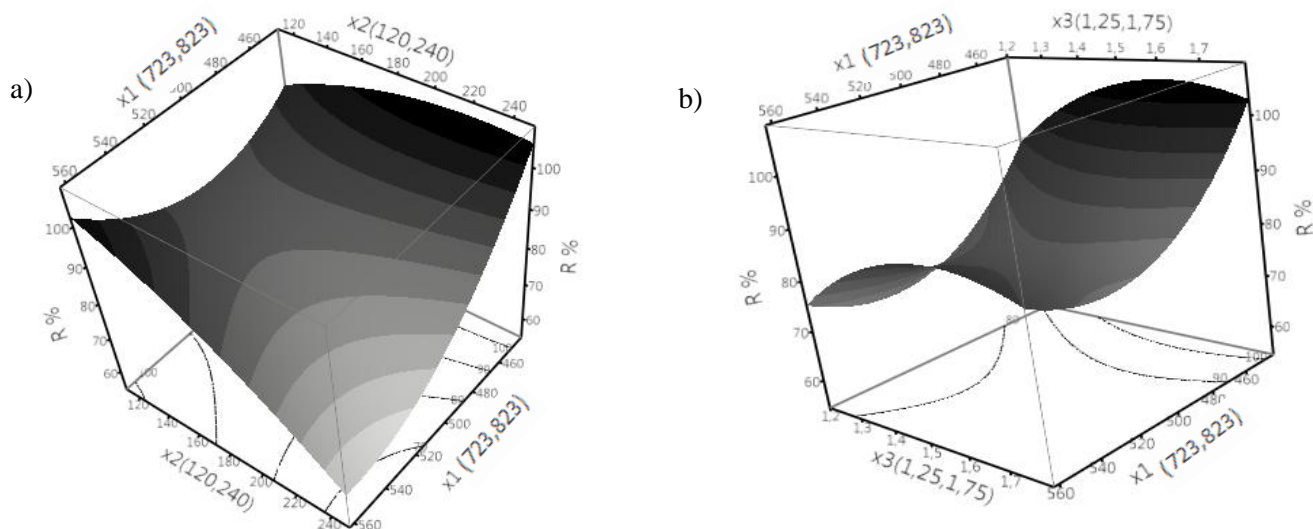


Figure 5. Three-dimensional response surface plots for yield of AC: effect of temperature and impregnation



**Figure 6.** Three-dimensional response surface plots for MB Removal of AC: (a) effect of time and temperature and (b) effect of temperature and impregnation ratio.

### 3.5. Raw pomegranate leaf and activated carbon characterization

#### 3.5.1. DRX analysis of activated carbon

From the XRD spectra of the activated carbon sample shown in Fig. 7. we can see exist two broad diffraction peaks located at  $2\theta = 20\text{--}30^\circ$  and  $40\text{--}50^\circ$ . Which could be attributed to the reflection from the (0 0 2) and (1 0 0) planes. These broad peaks are the characteristics of amorphous carbon with carbon ring that disorderly stack up. Thus, the activated carbon obtained can be identified as the carbon with amorphous structure [31 and 32].

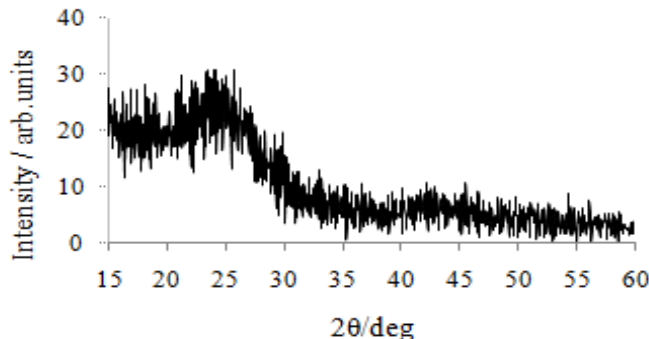


**Figure 7.** XRD Pattern of Activated Carbon

#### 3.5.2. FTIR analysis of precursor and activated carbon prepared

Fig. 8 illustrate the FTIR spectrum of the raw pomegranate leaf and the activated carbon prepared. The raw pomegranate leaf shows indications of various surface functional groups. The wide peak, which located at around  $3394\text{ cm}^{-1}$  is typically attributed to hydroxyl groups or/and adsorbed water. The bands located at  $2936$  and  $2858\text{ cm}^{-1}$  correspond to C–H vibrations of methyl and methylene groups [33]. The band at  $2368\text{ cm}^{-1}$  is characteristic of the  $\text{C}\equiv\text{C}$  stretching vibration of alkyne groups [34–37]. The band around  $1700\text{ cm}^{-1}$  is usually caused by the stretching vibration of  $\text{C}=\text{O}$  carboxyl groups. While the band around  $1600\text{ cm}^{-1}$  is ascribed to the aromatic ring or  $\text{C}=\text{C}$  stretching vibration [38]. The peak at  $1570\text{ cm}^{-1}$  represented the C–C stretching of aromatic rings. The bands at around  $1458$  and  $1386\text{ cm}^{-1}$  corresponded to the C–H in-plane bending vibrations in methyl and methylene groups [39]. The appearance of a band at  $1344\text{ cm}^{-1}$  can be attributed to C–O stretching vibrations in carboxylate groups. The band at  $1236\text{ cm}^{-1}$  and a relatively intense band at about  $1052\text{ cm}^{-1}$  can be assigned to C–O stretching vibrations in alcohols, phenols, or ether or ester groups. The C–H out-of-plane bending vibrations in benzene derivative cause the bands at  $886$  and  $838\text{ cm}^{-1}$ . Finally, the band caused by O–H out-of-plane bending vibrations band is located at  $608\text{ cm}^{-1}$ . [34 and 40].

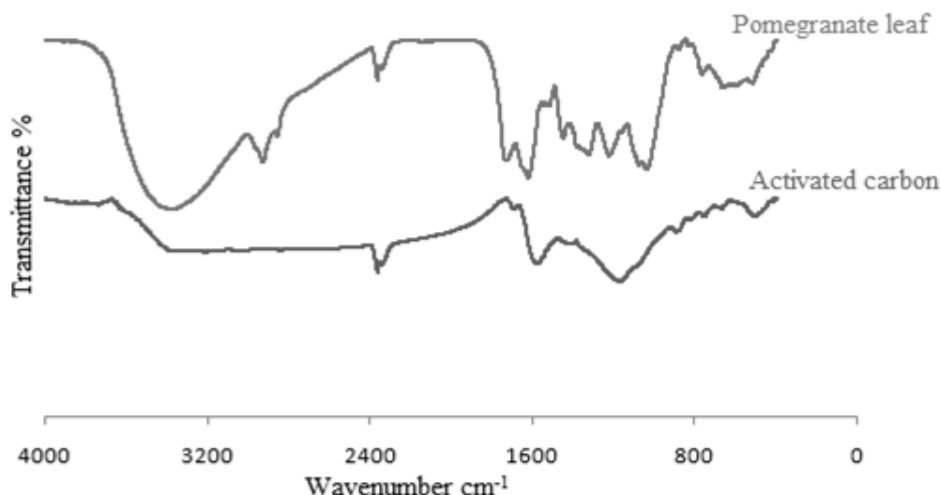


**Figure 8.** FTIR spectra of Pomegranate leaf and Activated carbon prepared.

The FTIR spectra of activated carbon prepared under the optimum conditions is also shown in Fig. 8. Fewer functional groups were detected, indicating that the surface functional groups of pomegranate leaf experienced chemical changes during pyrolysis. Compared with the precursor, the C–H vibrations in methyl and methylene groups at 2936 and 2858 cm<sup>-1</sup>, disappears with the thermal treatment. The peaks at 1740 cm<sup>-1</sup> and 1630 cm<sup>-1</sup>, are observed in the starting material, belonging respectively to carbonyl groups and C=C stretching vibration or to the aromatic ring become much weaker after activation, suggesting the carbonization of the material is almost complete [34]. The strong band located at approximately 1162 cm<sup>-1</sup> can be attributed to the stretching vibration of hydrogen-bonded P=O groups from phosphates or polyphosphates, the O–C stretching vibration in the P–O–C linkage and P=OOH [33, 41 and 42]. The surface chemistry of the activated carbon was different from the raw pomegranate leaf as many of the functional groups disappeared after carbonization and activation processes. This was due to the thermal degradation effect during the carbonization and activation processes which resulted in the destruction and formation of some intermolecular bondings [15].

### 3.5.3. TG and DTA analysis

Thermoanalytical techniques such as DTA and TG have been widely used to study the thermal behavior of agricultural products [43]. The thermogravimetric curves (Fig.9) indicates a complete evaporation process. Like all vegetable biomass, pomegranate leaf is composed of cellulose, hemi-cellulose and lignin [39].

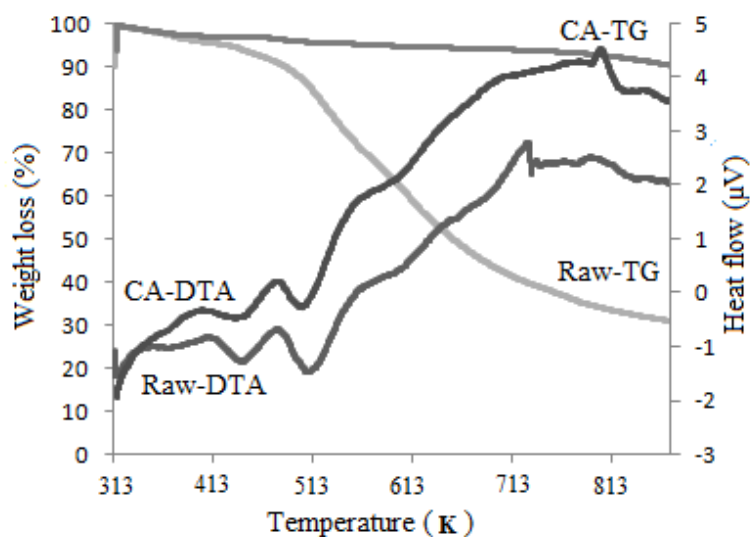


**Figure 9.** Thermo gravimetric and differential thermal analysis (TG-DTA) curves of pomegranate leaves

The moisture drying region corresponds to an initial slight weight loss 4% between ambient temperature and nearly 378 K, which results from the elimination of physically absorbed water in Pomegranate leaf and superficial or external water bounded by surface tension [44 and 45]. This explains the origin of the exothermic behavior at temperature below 373 K (see DTA curve, Fig. 4). The second stage of 413 – 733 K, which has a major weight loss 66%, corresponds to primary carbonization or active pyrolysis. This considerably greater weight loss is due to the elimination of volatile matters, tars, CO, CO<sub>2</sub> and Steam, ...etc.

This stage can be divided in two parts corresponding to the decomposition of hemicelluloses (413 - 563 K), associated to a 24% weight loss. Following, one contiguous and/or simultaneous process between 563 and 733 K, with a 32% weight loss, is ascribed to the cellulose degradation. Finally, a prolonged weight loss of 11%, in the 733 – 873 K range, might be attributed to the last stage of degradation of lignin. Among the three components, lignin was the most difficult one to decompose. Its decomposition happened slowly under the whole temperature range from ambient even above 873 K [46 - 50].

In summary, during the pyrolytic process of the precursor up to 873 K, around 71% of the ligno-cellulosic biomass can be volatilized, with a 29% of residual materials, besides about 4% of water.

In the Thermo gravimetric curve of activated carbon the first weight loss around 373 K observed was probably caused by the thermodesorption of water vapour. The activated carbon is thermally stable up to 873 K. Enhancement in the thermal stability is observed upon activation. As explained above for the precursor, the overall mass loss during the differential thermal analysis of activated carbon can be divided into steps related to moisture: hemi-cellulose, cellulose and lignin [39].

#### 3.5.4. Specific surface area and N<sub>2</sub> adsorption-desorption isotherms of AC prepared

One of the most important features of adsorbents is their surface area and porosity [10]. And the Brunauer-Emmett-Teller (BET) gas adsorption method has become the most widely used standard procedure for the determination of the surface area [51]. The BET surface area of activated carbon was found to be 193.62 m<sup>2</sup>/g with a total pore volume of 0.2743 cm<sup>3</sup>/g and an average pore diameter of 2.42 nm, indicating essentially a mesoporous nature. Basically, the structures of activated carbons are classified according to the International Union of Pure and Applied Chemistry (IUPAC) into three groups: micropore (diameter < 2 nm), mesopore (2-50 nm) and macropore (>50 nm) [33].

The porous properties of activated carbon elaborated from pomegranate leaves were determined from N<sub>2</sub> adsorption experiments. Figure 10 depicts the nitrogen adsorption/desorption isotherms.

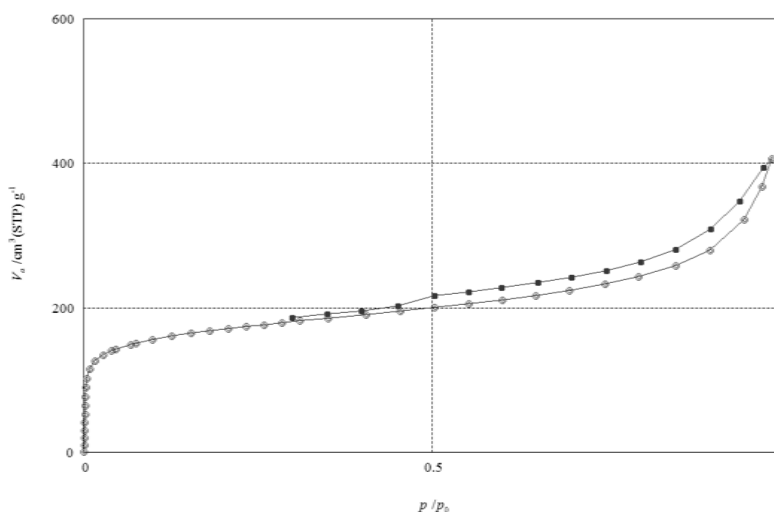


**Figure 10.** N<sub>2</sub> adsorption–desorption isotherm of AC at 77 K

The isotherms of AC presented both type I and type IV curves according to IUPAC classification at intermediate and high relative pressures. In initial part, it is of type I with an important uptake at low relative pressures characteristic of microporous materials. However, the knee of the isotherms is wide no clear plateau is attained and a certain hysteresis slope can be observed at intermediate and high relative pressures. All these facts indicating the presence of large micropores and mesopores (type IV) [52 and 53].

### 3.5.5. Surface morphology

The morphology of activated carbon was analyzed using Scanning Electron Microscopy (SEM).

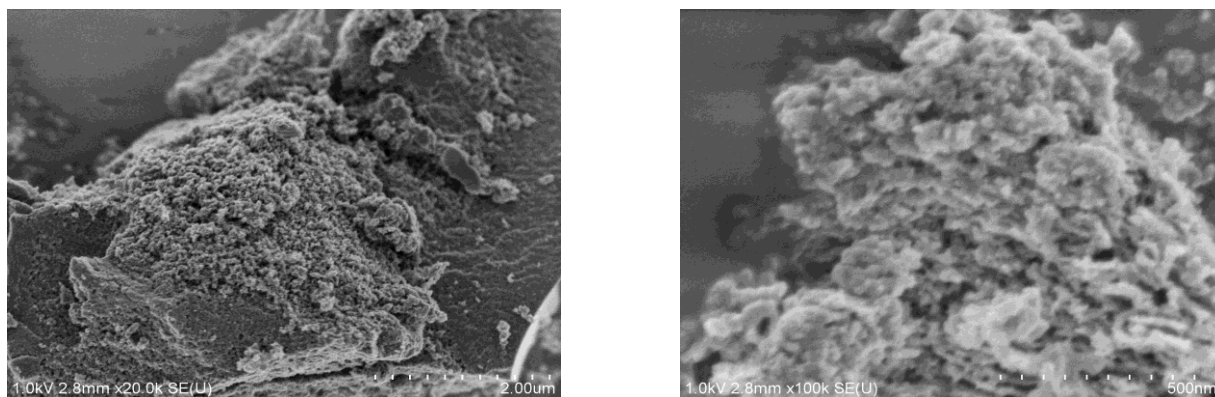


**Figure 11.** SEM image of Pomegranate Leaves activated carbon prepared under optimum conditions

SEM images of the resultant activated carbon prepared based on the activation temperature (723 K) activation time (2 h 24 min) and impregnation ration (1.45) are shown in figure 11. It can be seen from these micrographs that the activated carbons have an irregular and heterogeneous surface morphology with a well-developed porous structure. Pores of different sizes shapes could be observed. The development of the pore system in carbon depends on the structure of the starting material and the activated process [38].

## Conclusion

Pomegranate Leaves were used as precursor to prepare activated carbon with high surface area, sufficient yield of carbon and high dye removal. A central composite design was successfully used to investigate the effects of activation temperature, activation time and impregnation ratio. On the percentage yield and removal of MB of the activated carbon prepared. The optimum activated carbon preparation conditions were obtained using 723K activation temperature, 2h24minactivation time and 1.45 IR resulting in 60.82 % of carbon yield and 96.76% of MB removal. Through analysis of the response surface, three variables studied were found to have significant effects on MB Removal. But extraction temperature was the most significant factor to affect this response. Impregnation ratio was found to have the greatest effect on carbon yield followed by extraction temperature. The activated carbon prepared demonstrated high surface area and well-developed porosity. Activated carbon was shown to be a promising adsorbent for removal of methylene blue from aqueous solutions with high yield. The advantage of using agricultural by-products as raw materials for manufacturing-activated carbon is that these raw materials are renewable and potentially less expensive to manufacture.

## References

1. ZIDANI L. *Université de Batna, Faculté des sciences exactes, Algerie.*
2. Baeissa E S. *J. Alloys Compd.* 590 (2014) 303-308.
3. Gleick P H. *Pacific Institute for Studies in Development, Environment, and Security.* (2002).
4. Han R. Wang Y. Han P. Shi J. Yang J and Lu Y. *J. Hazard. Mater. B* 137 (2006) 550-557.
5. Mitrogiannis D. Markoua G. Çelekli A and Bozkurt H. *J. Environ. Chem. Eng.* 3 (2015) 670-680.
6. J M Salman. *J. Chem.* (2013) 1-6.
7. Saucier C. Adebayo M A. Lima E C. Cataluña R. Thue P S. Prola L D T. Puchana Rosero M J. Machado F M. Pavan F A and Dotto G L. *J. Hazard. Mater.* 289 (2015) 18-27.
8. Ahmad M A and Alrozi R. *Chem. Eng. J.* 165 (2010) 883-890.
9. Idris M N. Ahmad Z A. Ahmad M A. Ahmad N and Sulaiman S K. *Int. J. Eng. Technol.* 11 (2011) 234-240.
10. Auta M and Hameed B H. *Chem. Eng. J.* 175 (2011) 233-243.
11. Bello O S and Ahmad M A. *Sep. Sci. Technol.* 46 (2011) 2367-2379.
12. Tarbaoui M. Oumam M. Fakhfakh N. El Amraoui B. Benzina M. Bennamara A. Charrouf M and Abourriche A. *Anal. Chem. Ind. J.* 15 (2015) 54-64.
13. Ghaedi A M. Ghaedi M. Vafaei A. Irvani N. Keshavarz M. Rad M. Tyagi I. Agarwal S and Gupta V K. *J. Mol. Liq.* 206 (2015) 195-206.

14. Cronjea K J, Chettya K, Carskya M, Sahuc J N and Meikap B C. *Desalination*. 275 (2011) 276-284.
15. Salman J M. *Arabian J. Chem.* 7 (2014) 101-108.
16. Sumathi S, Bhatia S, Lee K T and Mohamed A R. *Bioresour. Technol.* 100 (2009) 1614-1621.
17. Issa A A, Al-Degs Y S, Al-Ghouti M A and Olimat A A M. *Chem. Eng. J.* 240 (2014) 554-564.
18. Ghaedi M and Kokhdan S N. *Spectrochim. Acta. Part A* 136 (2015) 141-148.
19. Son J, Vavra J, Li Y, Seymour M and Forbes V. *Chemosphere* 124 (2015) 136-142.
20. Amyrgialakia E, Makris D P, Mauromoustakos A and Kefalas P. *Ind. Crops Prod.* 59 (2014) 216-222.
21. Hang Y, Qu M and Ukkusuri S. *Energy and Buildings* 43 (2011) 988-994.
22. Goupy J et Creighton L. *Introduction aux plans d'expériences (3ème édition)*. DUNOD. Paris. 179-180 (2006).
23. Khuri A L. *Response Surface Methodology and Related Topics*. World scientific publishing. p. 23 (2006).
24. Amin N K. *J. Hazard. Mater.* 165 (2009) 52-62.
25. Chowdhury Z.Z, Zain S.M, Khan R.A, Ahmad A.A, Khalid K., *Res. J. Appl. Sci. Eng. Technol.* 4 (2012) 458
26. Quinn G P and Keough M J. *Experimental Design and Data Analysis for Biologists*. Cambridge University Press. p 173 (2002).
27. Tan I A W, Ahmad A L and Hameed B H. *J. Hazard. Mater.* 153 (2008) 709-717.
28. Noordin M Y, Venkatesh V C, Sharif S, Elting S, Abdullah A. *J. Mater. Process. Technol.* 145 (2004) 46.
29. Proust M. *JMP Statistics and Graphics Guide, Release 7*. SAS Institute Inc., Cary, NC, USA (2007)
30. Zhu C and Liu X. *Carbohydr. Polym.* 92 (2013) 1197-1202.
31. Tang Y-b, Liu Q and Chen F-y. *Chem. Eng. J.* 203 (2012) 19-24.
32. Bohli T, Ouederni A, Fiol N and Villaescusa I. *C. R. Chim.* 18 (2015) 88-99.
33. Kaouah F, Boumaza S, Berrama T, Trari M and Bendjama Z. *J. Clean. Prod.* 54 (2013) 296-306.
34. Yang J and Qiu K. *Chem. Eng. J.* 165 (2010) 209-217.
35. Shaarani F W and Hameed B H. *Chem. Eng. J.* 169 (2011) 180-185.
36. Ceyhan A A, Sahin Ö, Baytar O and Saka C. *J. Anal. Appl. Pyrol.* 104 (2013) 378-383.
37. Anisuzzaman S M, Joseph C G, Taufiq-Yap Y H, Krishnaiah D and Tay V V. *J. King Saud Univ. Sci.* in press (2015).
38. Shi Q, Zhang J, Zhang C, Li C, Zhang B, Hu W, Xu J and Zhao R. *J. Environ. Sci.* 22 (2010) 91-97.
39. Liu L, Liu J, Li H, Zhang H, Liu J and Zhang H. *Bioresources* 7 (2012) 3555-3572.
40. Lua A C and Yang T. *J. Colloid. Interf. Sci.* 276 (2004) 364-372.
41. Kılıc M, Apaydın-Varol E and Pütün A E. *Appl. Surf. Sci.* 261 (2012) 247-254.
42. Stuart B. *Infrared Spectroscopy: Fundamentals and Applications*. John Wiley & Sons Ltd, England. p. 85 (2004).
43. Ozdemira M, Bolgaza T, Sakab C and Şahin O. *J. Anal. Appl. Pyrol.* 92 (2011) 171-175.
44. Chen G, Du G, Ma W, Yan B, Wang Z and Gao W. *Fuel* 144 (2015) 214-221.
45. Anirudhan T S and Sreekumari S S. *J. Environ. Sci.* 23 (2011) 1989-1998.
46. Hadouna H, Sadaouib Z, Souamia N, Sahel D and Toumert I. *Appl. Surf. Sci.* 280 (2013) 1-7.
47. Haykiri-Acma H, Yaman S and Kucukbayrak S. *Fuel Process. Technol.* 91 (2010) 759-764.
48. Lopez-Velazquez M A, Santesa V, Balmasedab J and Torres-Garcia E. *J. Anal. Appl. Pyrol.* 99 (2013) 170
49. Khezami L, Chetouani A, Taouk B and Capart R. *Powder Technol.* 157 (2005) 48-56.
50. Yang H, Yan R, Chen H, Lee D H and Zheng C. *Fuel* 86 (2007) 1781-1788.
51. Sing K S W, Everett D H, Haul R A W, Moscou L, Pierotti R A, Rouquerol J And Siemieniewska T. *Pure Appl. Chem.* 57 (1985) 603-619.
52. Passe-Coutrin N, Altenor S, Cossement D, Jean-Marius C and Gaspard S. *Microporous Mesoporous Mater.* 111 (2008) 517-522.
53. Gao Y, Yue Q, Xu S, Gao B, Liand Q and Yu H. *Chem. Eng. J.* 274 (2015) 76-83.

(2016) ; <http://www.jmaterenvirosci.com/>